Single-crystal NMR for the layered semiconductor $TlGaSe_2$

2008 J. Phys.: Condens. Matter 20 395211

(http://iopscience.iop.org/0953-8984/20/39/395211)

J. Phys.: Condens. Matter **20** (2008) 395211 (8pp) doi:10.1088/0953-8984/20/39/395211

Single-crystal NMR for the layered semiconductor $TlGaSe_2$

A M Panich[1,3] **and S Kashida**[2]

[1] Department of Physics, Ben-Gurion University of the Negev, PO Box 653, Beer-Sheva 84105, Israel
[2] Department of Environmental Science, Faculty of Science, Niigata University, Ikarashi-ninocho 8050, Niigata 950-2181, Japan

E-mail: pan@bgu.ac.il

Received 6 April 2008, in final form 13 August 2008
Published 1 September 2008
Online at stacks.iop.org/JPhysCM/20/395211

Abstract

We report on a ^{69}Ga and ^{205}Tl NMR study of single-crystal thallium gallium selenide. Our findings show that transformation from the high temperature paraelectric phase to the low temperature ferroelectric phase occurs via an incommensurate phase that exists in the temperature range from $T_c = 107.5$ to $T_i = 118$ K. On approaching phase transition at T_i from above, the crystal exhibits soft mode behavior, which is somewhat different for thallium and gallium substructures. Redistribution of ^{69}Ga line intensities with temperature in the ferroelectric phase indicates a variation of the domain structure of this phase.

(Some figures in this article are in colour only in the electronic version)

1. Introduction

The ternary chalcogenide $TlGaSe_2$ is a quasi-two-dimensional compound whose structure consists of layers formed by corner-linked $GaSe_4$ tetrahedra and Tl^{1+} ions located on straight lines between the layers [1–3] (figure 1). Two adjacent layers and chains are turned relative to each other by 90°. Under ambient conditions, the structure has monoclinic symmetry, the space group is $C2/c - C_{2h}^6$, $a = 10.772$ Å, $b = 10.771$ Å and $c = 15.636$ Å, $\beta = 100.6°$, $Z = 16$ [1–3] and it exhibits two Ga, two Tl and five Se sites. The compound is of interest due to low dimensionality, semiconducting and photoconducting properties, negative differential resistance in the I–V characteristics, memory effects and optical second harmonic generation [4–11]. Sub-millimeter dielectric spectroscopy measurements by Volkov *et al* [12, 13] showed that $TlGaSe_2$ exhibits successive phase transitions at ∼107 and ∼120 K with an intermediate phase that was assumed to be incommensurate. Dielectric measurements [14] revealed the ferroelectric character of the low temperature phase and the paraelectric character of the high temperature phase. Volkov *et al* [12] have shown that $TlGaSe_2$ exhibits soft mode behavior that is typical of displacive-type ferroelectrics. X-ray diffraction measurements in a single crystal of $TlGaSe_2$ [15] revealed that the phase between 117 and 110 K is incommensurate and characterized by a modulation wavevector (δ, δ, 1/4), where $\delta \approx 0.02$ in reciprocal lattice units. A later single-crystal neutron scattering study of $TlGaSe_2$ by Kashida *et al* [16] showed the existence of an incommensurate state between 107 and 118 K with a modulation wavevector (δ, 0, 1/4), where $\delta = 0.04$. In the low temperature phase, the satellite reflections appear at the commensurate position $q_c = (0, 0, \pm 0.25)$ [16], indicating a quadrupling of the unit cell along the c-axis compared to that of the high temperature phase. This phase was assigned to the space group Cc [14].

Phase transition temperatures in $TlGaSe_2$, reported by different authors, are usually found between 107–110 K and 117–120 K, respectively [12–17]. However, Allakhverdiev *et al* [18], Aldzhanov *et al* [19] and Mikailov *et al* [20] detected the third phase transition around 100–103 K by means of heat capacity and dielectric measurements and interpreted it as a final lock-in transition accompanied by the formation of the ferroelectric state in $TlGaSe_2$. Furthermore, some authors reported phase transitions at 200–215 K [21] and 240–250 K [18, 19, 22]. Thus the literature data on phase transitions and incommensurability in $TlGaSe_2$ are somewhat inconsistent.

In the present paper we report on a NMR study of single-crystal $TlGaSe_2$. This investigation showed that the

[3] Author to whom any correspondence should be addressed.

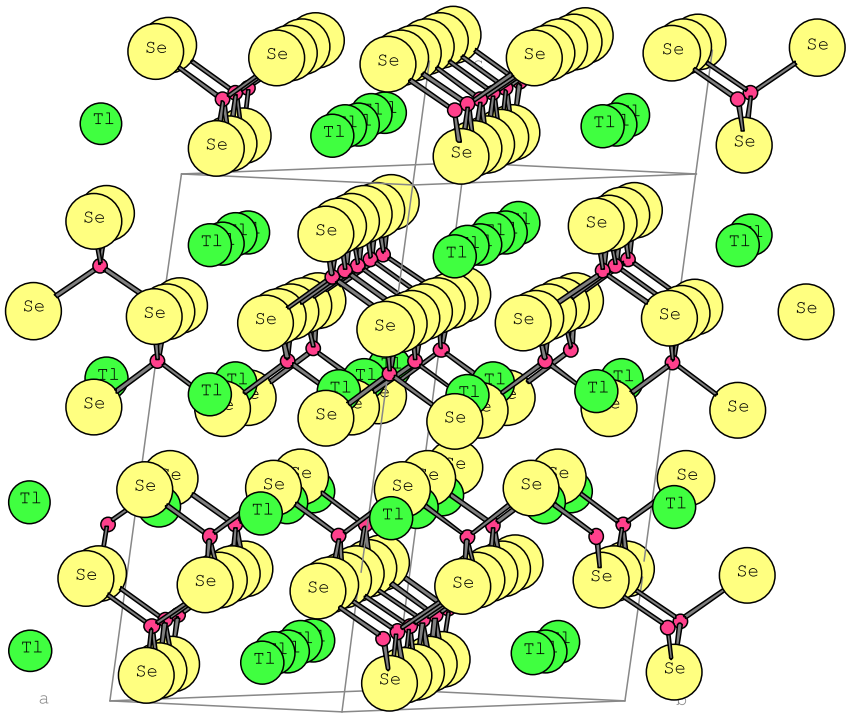

Figure 1. Structure of $TlGaSe_2$ comprises layers in the a, b plane. Tl^{1+} ions are located between layers on straight lines along [1, 1, 0] and [1, $\bar{1}$, 0] directions (at different height along the c-axis). Ga atoms are shown by small circles.

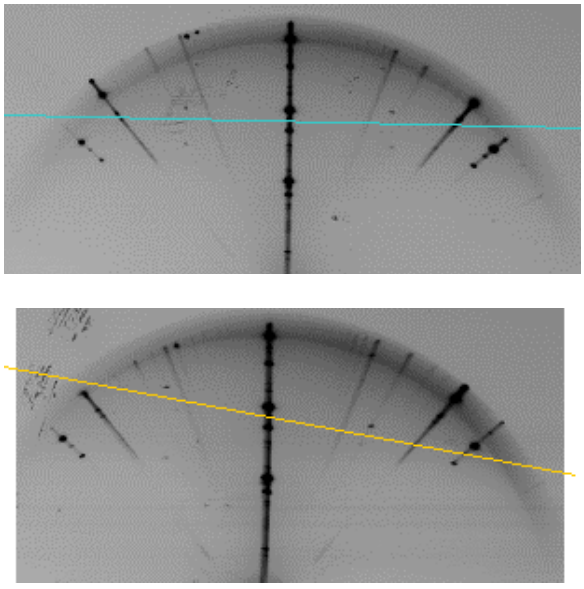

Figure 2. Precession x-ray photographs of the $TlGaSe_2$ single crystal. Top: the [100] zone; the c^*-axis is vertical and the b^*-axis is a horizontal line. Bottom: the [010] zone; the c^*-axis is vertical and the a^*-axis is an oblique line.

transformation from the high temperature paraelectric phase to the low temperature ferroelectric phase occurs via an incommensurate phase that exists in the temperature range from $T_c = 107.5$ to $T_i = 118$ K. (Here and later we use the generally accepted designations of T_i for a high temperature normal–incommensurate transition and T_c for a low temperature 'lock-in' transition to a commensurate phase.) Redistribution of ^{69}Ga line intensities with temperature in the ferroelectric phase allows us to suggest that this phase exhibits domain structure. On approaching the phase transition at T_i from above, the crystal exhibits soft mode behavior, which is different for Tl and Ga substructures. The behavior of the magnetization recovery of ^{69}Ga at 118–128 K differs from that at higher temperatures. The ^{205}Tl spectrum transforms from doublet to triplet around 220 K. The aforementioned transformations seem not to be characteristic of the phase transitions, and their origin is discussed in the paper.

2. Experimental details

The single crystal of $TlGaSe_2$ was grown by the Bridgman method. It is a parallelepiped of 10 mm × 3 mm × 1 mm in size with the c^*-axis perpendicular to the crystal plane. X-ray photographs (figure 2) showed that the crystal has monoclinic symmetry and is not a twin. ^{205}Tl and ^{69}Ga NMR spectra and spin–lattice relaxation times T_1 were measured using a Tecmag Apollo pulse NMR spectrometer, an Oxford Instruments cryostat and an Oxford superconducting magnet (external magnetic field $B_0 = 8.0196$ T) in the temperature range 80–295 K. The spectra were obtained using the Hahn echo ($\pi/2 - \tau - \pi$) pulse sequence with phase cycling. The T_1 values of each isotope were measured by means of a saturation comb sequence. The durations of the $\pi/2$ pulse were 2.3 μs for ^{69}Ga and 2 μs for ^{205}Tl.

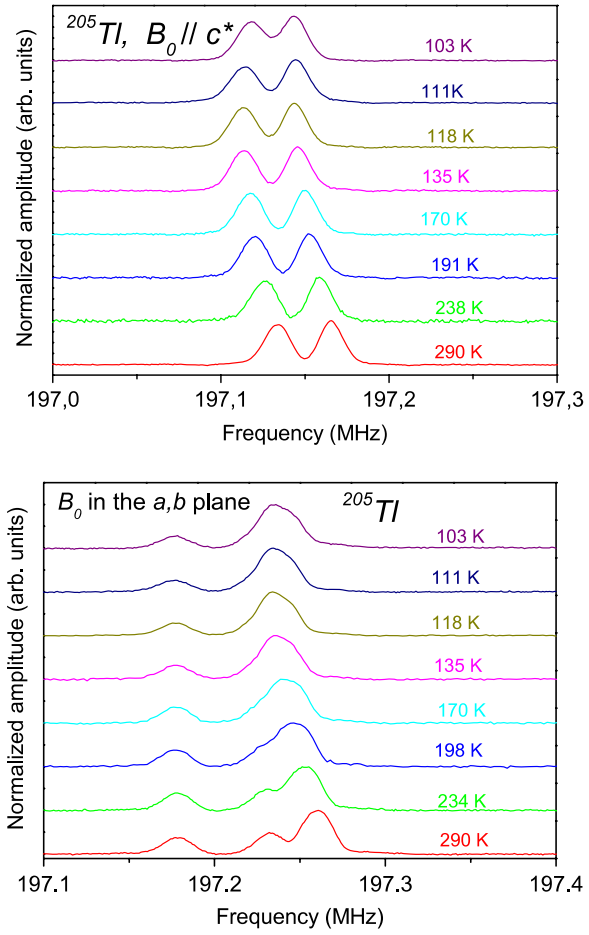

Figure 3. ^{205}Tl NMR spectra at different temperatures for $B_0 \parallel c^*$ (top) and $B_0 \perp c^*$ (bottom).

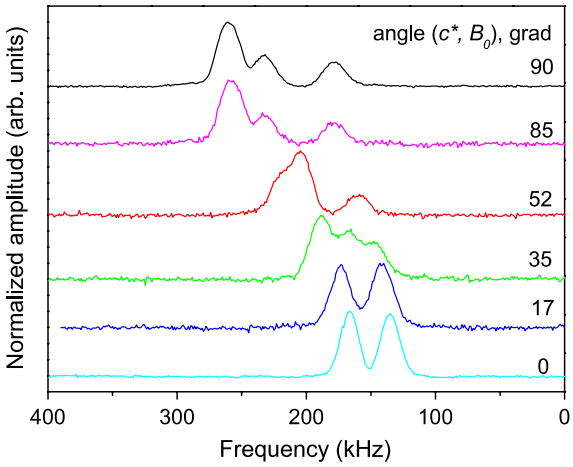

Figure 4. Angular dependence of the ^{205}Tl NMR spectra at $T = 293$ K. The scale starts from the frequency 197 MHz.

3. Results of the experiments

3.1. Thallium NMR spectra and spin–lattice relaxation

The isotope ^{205}Tl has spin $I = 1/2$. ^{205}Tl NMR spectra at different temperatures and at two orientations of the applied magnetic field B_0 with respect to the crystal axes are shown in figure 3. The angular dependence of the room temperature spectra is presented in figure 4. When the external magnetic field B_0 is applied along the c-axis, the spectra show two ^{205}Tl resonances of nearly equal intensities in the whole temperature range. These lines come from the two structurally inequivalent Tl atoms in the $TlGaSe_2$ structure, Tl1 and Tl2, which exhibit different chemical shielding components $\sigma_\parallel$. However, when we apply a magnetic field B_0 in the a, b plane, the low temperature spectra ($T < 200$ K) show two lines with an intensity ratio around 3:1. Furthermore, heating the sample above $T \sim 220$ K causes line splitting, resulting in a gradual transformation of the two-component spectrum into the three lines with an intensity ratio around 2:1:1 at room temperature. The line positions in the NMR spectra of ^{205}Tl ($I = 1/2$) are determined by the chemical shifts of Tl nuclei; thus the number of magnetic resonance lines in the spectrum is determined by the number of physically inequivalent nuclei in the unit cell. We note that one should distinguish between crystallographically inequivalent sites, where chemical shielding tensors have different principal values and different orientations of the principal axes in the unit cell, and physically inequivalent sites, where chemical shielding tensors have the same principal values but different orientations of the principal axes with respect to the applied magnetic field. While $TlGaSe_2$ has two structurally inequivalent Tl sites, it shows four physically inequivalent Tl sites because of the existence of perpendicular Tl chains in the a, b plane. Each chain comprises two non-equivalent Tl atoms. When a magnetic field is applied along the c-axis, it forms the same angle of 90° with each chain, making them equivalent, and we observe two signals coming from two inequivalent Tl atoms showing different values of $\sigma_\parallel$. However, when the magnetic field B_0 is in the a, b plane (figure 3, bottom), it generally forms different angles with the perpendicular chains, making them inequivalent. Since the chemical shift is angle dependent, one could generally observe four signals coming from two inequivalent Tl atoms in the first chain and from two inequivalent Tl atoms in the second (perpendicular) chain. However, due to the exchange interaction between Tl spins [23–34] two signals, whose chemical shifts are close to each other, collapse into one signal, revealing more intense line. Thus we would observe three lines with a 2:1:1 intensity ratio. We note that the observed chemical shifts of the Tl resonances are in the range of such shifts in the other Tl compounds [23–34], and that the obtained chemical shielding anisotropy is evidently caused by a non-spherical surrounding of Tl atom by six Se atoms, forming a non-spherical electronic shell of Tl.

Temperature dependences of the ^{205}Tl resonance frequencies are shown in figure 5. The aforementioned doublet–triplet transformation at $T \sim 220$ K is clear with $B_0 \perp c^*$. We note that the line shape analysis shows no noticeable broadening on cooling. In fact, the observed effect is caused by a reduction of the resonance frequency of the high frequency line on cooling that is evident in figure 3 (bottom) and figure 5 (bottom), so that this line (at 197.26 MHz) approaches the line at 197.23 MHz, finally causing two resonances to overlap and to

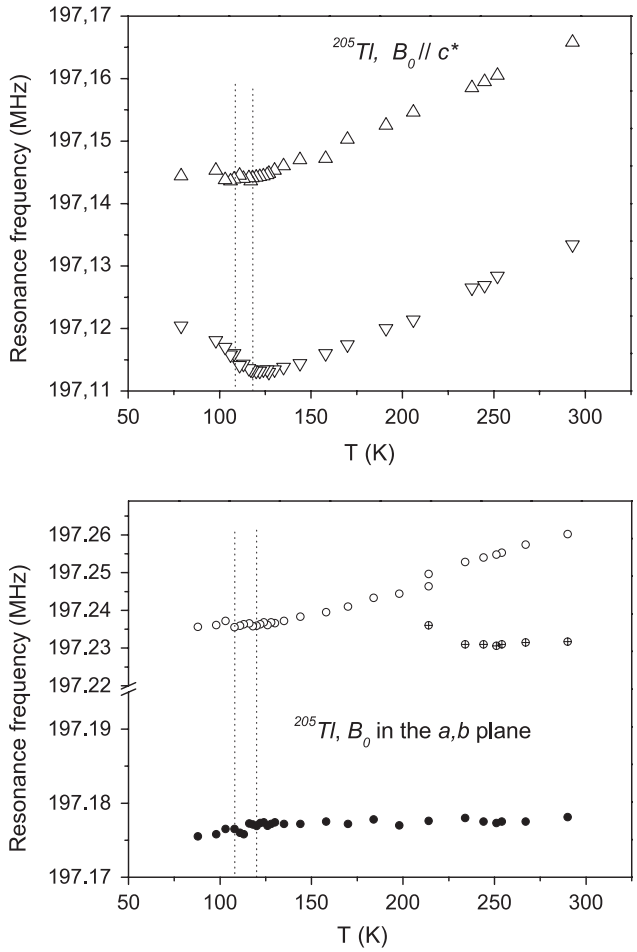

Figure 5. Temperature dependence of the ^{205}Tl resonance frequencies for $B_0 \parallel c^*$ (top) and $B_0 \perp c^*$ (bottom). Dotted lines show phase transition temperatures.

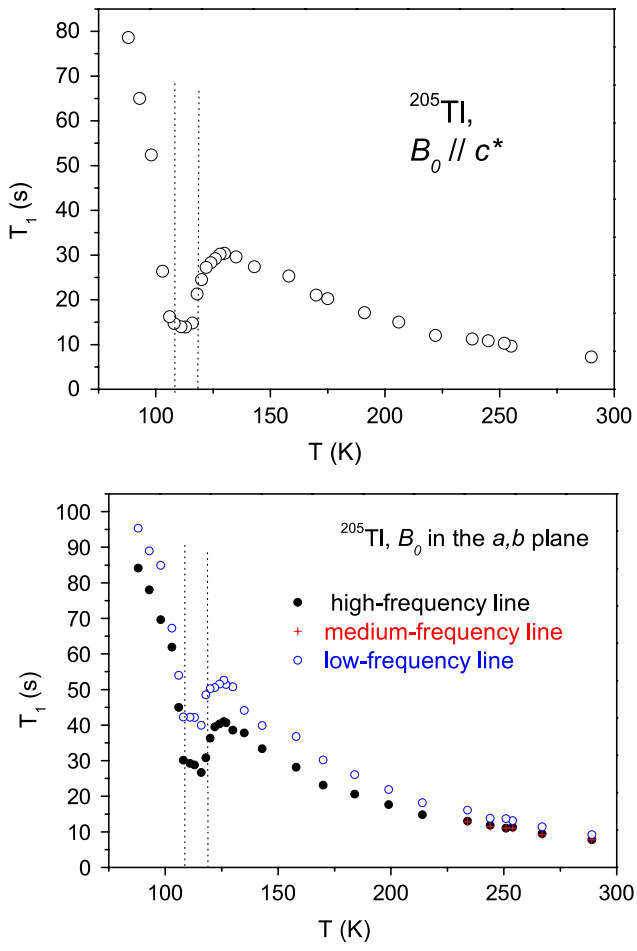

Figure 6. Temperature dependence of the ^{205}Tl spin–lattice relaxation time T_1 for $B_0 \parallel c^*$ (top) and $B_0 \perp c^*$ (bottom). The values of T_1 for high and low frequency resonances at $B_0 \parallel c$ were found to be practically the same. Dotted lines show phase transition temperatures.

be unresolved. Such behavior is not characteristic of phase transition. We note, however, that Abutalybov *et al* [21], who measured photoconductivity and optical spectra in $TlGaSe_2$, reported on some anomalies assigned to an eventual phase transition around 200–215 K.

Below $T \sim 220$ K the resonance frequencies of the ^{205}Tl signals for both orientations, $B_0 \parallel c^*$ and $B_0 \perp c^*$, vary slightly and more or less synchronously on cooling down to $T = 118$ K due to some temperature dependence of the chemical shielding tensor components $\sigma_\parallel$ and $\sigma_\perp$. However, the character of these variations changes below 118 K, which is particularly seen for the low frequency resonance at $B_0 \parallel c^*$. At the same time, the line shape remains practically the same, except for some broadening on cooling. The above transformations allow one to speculate that they are accompanied by a displacement of the Tl atoms. On the other hand, the phase transitions may also be caused by some deformation of the $GaSe_4$ tetrahedra, which, in turn, can 'drag' the Tl atoms due to existence of a weak Tl–Se–Ga bond [23, 24]. Such a bond, formed due to sp-hybridization of the Tl wavefunctions and their overlap with the Se p-orbitals [23, 24, 35], causes deviation of the Tl electron cloud from the spherical form and results in the chemical shielding anisotropy observed in the experiment (figure 4). Generally, variation of the NMR chemical shift of a given element results from the paramagnetic contribution to the chemical shielding σ_p, which is different from zero only for a nonzero angle θ between the applied magnetic field B_0 and the bond direction [36–38] and usually shows $\sigma_\perp$ in the high frequency extreme and $\sigma_\parallel$ in the low frequency extreme [36, 38], just as observed in our experiment (figure 4). This fact is consistent with the shorter distances from the Tl atom to the Ga–Se layer in the c^* direction than those in the a, b plane.

Temperature dependences of the ^{205}Tl spin–lattice relaxation times are shown in figure 6. The $T_1(T)$ plots exhibit three anomalies at 107.5, 118 and around 128 K (figure 6). Below $T = 107.5$ K, the spin–lattice relaxation time T_1 is decreased on heating as usual. In the range from 107.5 to 118 K, T_1 is short and nearly temperature independent (particularly for $B_0 \parallel c^*$) that is characteristic of the incommensurate state [39, 40]. Our data agree well with literature values, where the phase between 107.5 and 118 K is assigned to the incommensurate state [12–16].

When B_0 is applied along the c-axis, the T_1 values of different lines (figure 6) are practically the same. When

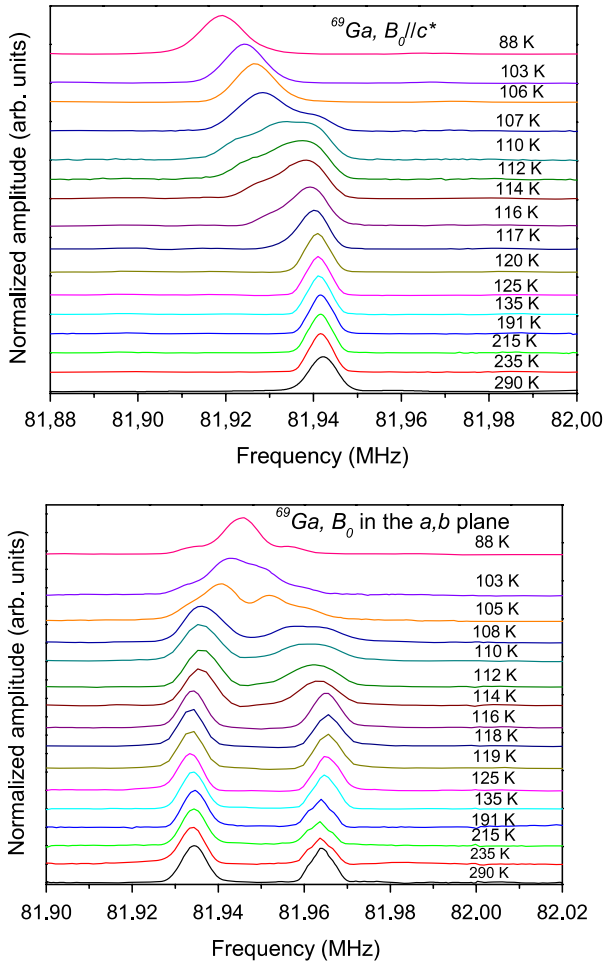

Figure 7. ^{69}Ga NMR spectra at different temperatures for $B_0 \parallel c^*$ (top) and $B_0 \perp c^*$ (bottom).

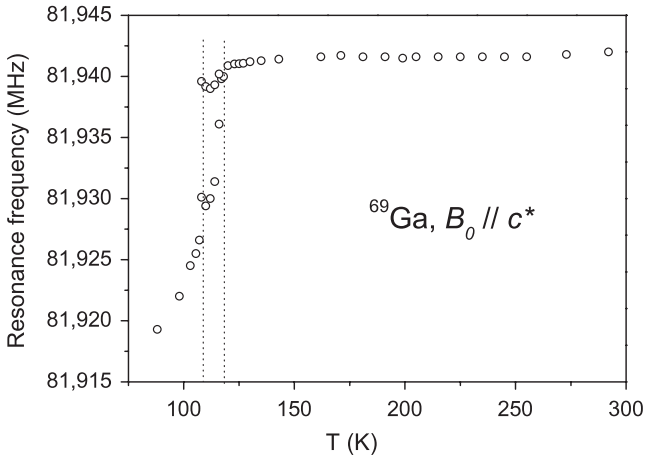

Figure 8. Temperature dependence of the ^{69}Ga resonance frequencies for $B_0 \parallel c^*$. The dotted lines show phase transition temperatures. In the temperature range from 107.5 to 118 K, the positions of two singularities are shown.

B_0 is in the a, b plane, the T_1 values of the two lines are different but show a very similar temperature dependence. The obtained dependences of T_1 mean that the mechanism of spin–lattice relaxation is similar for all Tl atoms and that the phase transitions at 107.5 and 118 K significantly affect the dynamics of the Tl sublattice. We note that the ^{205}Tl spectrum transformation around 220 K is not accompanied by visible changes in the temperature dependent T_1 measurements.

Above 118 K, T_1 demonstrates noticeable elongation on heating and reaches a maximum at ∼128 K, showing a drastic change (from plus to minus) in the sign of the slope of the $T_1(T)$ curve. At first sight, such a behavior may be attributed to a phase transition. We will discuss this effect in more detail in section 4 and will show that this is not the case.

3.2. Gallium NMR spectra and spin–lattice relaxation

^{69}Ga is a quadrupolar nucleus having spin $I = 3/2$. ^{69}Ga NMR spectra of the $TlGaSe_2$ single crystal for the central $1/2 \rightarrow -1/2$ transition are given for different temperatures and two orientations of the applied magnetic field B_0 in figure 7. The temperature dependence of the resonance frequency for one of the orientations is shown in figure 8.

When the applied magnetic field B_0 is in the a, b plane, we observe two ^{69}Ga resonances with nearly equal intensities, evidently coming from the two inequivalent Ga sites in the $TlGaSe_2$ structure [2, 3]. These sites presumably exhibit (i) different chemical shielding and (ii) different electric field gradients resulting in different second-order quadrupole shifts of the Ga resonances. The latter mechanism should reveal the difference in the observed splittings $\Delta\nu$ for ^{69}Ga and ^{71}Ga isotopes due to the difference in their quadrupole moments, $Q(^{69}\text{Ga}) = 168$ mb and $Q(^{71}\text{Ga}) = 106$ mb, respectively, and should therefore yield the ratio of these splittings to be $\Delta\nu(^{69}\text{Ga})/\Delta\nu(^{71}\text{Ga}) = [\nu_0(^{71}\text{Ga}) \times Q^2(^{69}\text{Ga})]/[\nu_0(^{69}\text{Ga}) \times Q^2(^{71}\text{Ga})] = 3.2$. Here $\nu_0(^{69}\text{Ga})$ and $\nu_0(^{71}\text{Ga})$ are the Larmor frequencies of the Ga isotopes. The experimentally measured $\Delta\nu(^{69}\text{Ga})/\Delta\nu(^{71}\text{Ga})$ ratio was found to be 2.3, which leads us to the conclusion of the mainly quadrupolar (∼72%) origin of this splitting; the rest is attributed to the difference in the chemical shielding of two Ga atoms.

When we apply the magnetic field B_0 along the c^* axis, a single ^{69}Ga resonance is observed, showing that the sum of the chemical shift and the quadrupolar shift components of two atoms in this direction coincide.

One can find that the ^{69}Ga spectra for both crystal orientations (figure 7) undergo visible variations in the temperature range 107.5–118 K, which was assigned to the incommensurate phase from the x-ray and neutron diffraction data [15, 16] and our ^{205}Tl NMR findings (section 3.1). For $B_0 \parallel c^*$, we observe that the single NMR resonance broadens and becomes asymmetric, showing a behavior that is characteristic of the incommensurate state, where the translational lattice periodicity is lost and there is an essentially infinite number of inequivalent sites contributing to the magnetic resonance spectrum. Thus the resonance frequency varies in space in a way that reflects the spatial variation of the incommensurate modulation [39, 40], and instead of a sharp line characteristic of commensurate crystals, the spectrum in the incommensurate phase is characterized by a quasi-continuous (inhomogeneous) distribution of the

NMR frequencies, just as observed in our experiment. On further cooling below $T_c = 107.5$ K, the spectrum gradually transforms into a symmetrical line. For $B_0 \perp c^*$ in the temperature range 107.5–118 K, both resonances broaden (figure 7), but this is more pronounced for the high frequency component. However, after transition into the low temperature ferroelectric phase, at $T < T_c$, the ^{69}Ga spectrum exhibits further variation and transformation from doublet to triplet on cooling down to ~100 K. Such a smooth evolution is not characteristic of a phase transition, and the redistribution of the ^{69}Ga line intensities in the ferroelectric phase with the variation of temperature may rather be caused by a domain structure of this phase, as discussed in the next section. We note that an analogous domain structure has been detected in the low temperature phase of the ferroelectric K_2SbF_5 [41].

Temperature dependences of the ^{69}Ga NMR spin–lattice relaxation times are collected in figure 9. The T_1 values of the single resonance at $B_0 \parallel c$ and those of high frequency resonance at $B_0 \perp c^*$ are close to each other in the whole temperature range under study, while the values of T_1 of the low frequency resonance at $B_0 \perp c^*$ are somewhat different. However, all resonances exhibit very short and nearly temperature independent relaxation in the range 107.5–118 K, with some decrease in T_1 on heating. Such a behavior is characteristic of the incommensurate state. More explicitly, spin–lattice relaxation is often due to phonon scattering processes. In incommensurate systems, the excitation spectrum consists of two modes [39, 40]: an optical-like amplitudon branch, $A = A_0 + \delta A(t)$, corresponding to oscillations of the amplitude of the modulation wave, and an acoustic-like phason branch, $\Phi = \Phi_0 + \delta\Phi(t)$, corresponding to oscillations of the phase of the modulation wave. The relaxation rate is proportional to the phason and amplitudon spectral densities at the Larmor frequency, respectively [39, 40]. The phason with wavevector q_I corresponds to the Goldstone mode that is gapless in the continuum limit, since the free energy of discommensuration does not depend on the phase of the modulation wave. The number of thermally excited phasons is of the order of acoustic phonons, but the relative nuclear displacements are not small since the wavevector $q_I \neq 0$. This leads to an extremely efficient spin–lattice relaxation mechanism for nuclei. We note that (i) the amplitudon contribution corresponds to a longer T_1 than does the phason and (ii) the relaxation time assigned to amplitudons increases as the temperature is lowered, whereas the phason contribution to T_1 is temperature independent [39, 40].

A comparison of the spin–lattice relaxation times for the two Ga isotopes shows that the ratio of $T_1(^{71}\text{Ga})/T_1(^{69}\text{Ga})$ is around 2.7, which is close to $[Q(^{69}\text{Ga})/Q(^{71}\text{Ga})]^2 = 2.51$, where Q is the nuclear quadrupole moment. This result is in accord with the well-known formula for quadrupolar relaxation [42] which assumes that the coupling of lattice vibrations with the quadrupole moment is the main relaxation mechanism for nuclear spins $I > 1/2$, as is usually the case. Andrew and Tunstall [43] have shown that for the quadrupolar mechanism of relaxation of nuclei with spin $I = 3/2$,

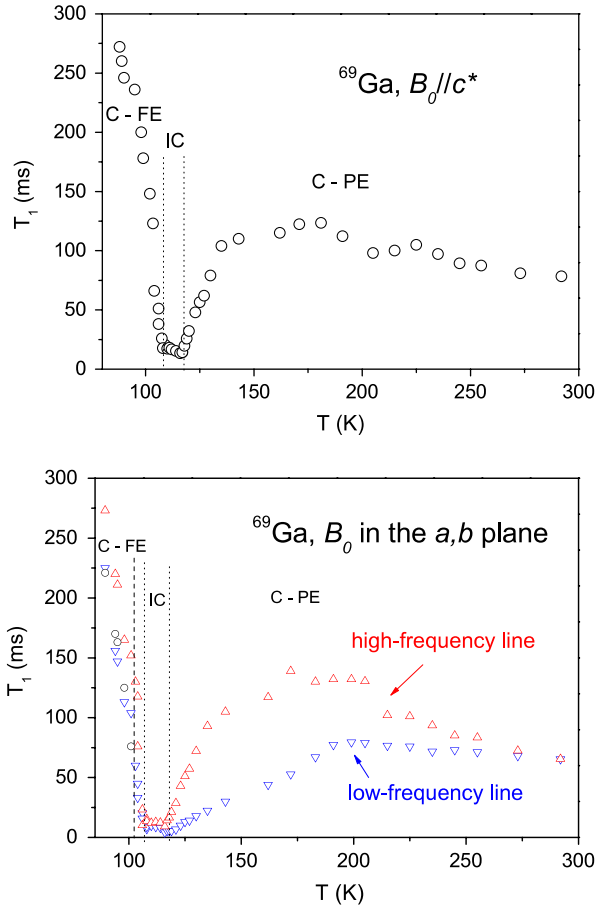

Figure 9. Temperature dependence of the ^{69}Ga spin–lattice relaxation time T_1 for $B_0 \parallel c^*$ (top) and $B_0 \perp c^*$ (bottom). The dotted lines show phase transition temperatures. The dashed line (bottom) indicates the approximate temperature of doublet-to-triplet transformation of the spectra at $B_0 \perp c^*$. C, IC, FE and PE denote commensurate, incommensurate, ferroelectric and paraelectric phases, respectively.

the magnetization recovery is generally described by the expression

$$1 - \left(\frac{W_2}{W_1 + W_2}\right)\exp(-2W_1 t) - \left(\frac{W_1}{W_1 + W_2}\right)\exp(-2W_2 t). \quad (1)$$

Here quantities W_1 and W_2 are a measure of the transition probabilities for $\Delta m = 1$ and 2, respectively.

However, quadrupole relaxation theories [44–47] and experiments [47–49] all lead to the view that W_1 and W_2 values are close to each other, thus a difference between two exponentials can hardly be distinguished. Such a behavior was observed in our experiment in the temperature range 130–290 K, where the magnetization recovery curve is well fitted by a single exponential. However, between 118 and ~128 K, on approaching the phase transition from the high temperature paraelectric phase to the incommensurate phase, ^{69}Ga nuclear magnetization recovery on measuring T_1 cannot be fitted by a single exponential. Since the W_1/W_2 ratio is not expected to be temperature dependent, the deviation from the single exponential at 118–128 K is unexpected.

In this temperature range, the magnetization recovery of each resonance is satisfactorily fitted by a stretched exponential:

$$M(t) = M(0)\{1 - \exp[-(t/T_1)^{\alpha}]\}. \quad (2)$$

It is known [50] that stretched exponential relaxation with the parameter α, varying in the range of $0 < \alpha < 1$, usually appears due to a distribution of the relaxation times arising in a system with a number of different relaxation environments. In the case in question, such a behavior of the spin–lattice relaxation between 118 and ∼128 K reflects a distribution of the correlation times of critical fluctuations on approaching the phase transition at T_i. This dynamic disorder indicates some inhomogeneity of the crystal. We note that the parameter α in equation (2) shows an increase from 0.7 to 1 on heating from 118 to 128 K, i.e. magnetization recovery becomes more exponential.

4. Discussion

First, let us discuss the ^{69}Ga spectrum transformation below the phase transition to the low temperature phase observed between ∼100 and 107.5 K. Since this transformation is smooth, and since the ^{69}Ga spin–lattice relaxation data in this temperature range do not exhibit an anomaly characteristic of phase transition, the origin of the aforementioned variations was presumed to be due to the domain structure of this phase. Indeed, as known, the free energy in the ferroelectric phase usually exhibits several minima that result in a domain structure. Domain redistribution on heating is likely to be accompanied by variations in the distribution of electric field gradients detected in the experiment. The observed variations probably lead to the corresponding changes in the heat capacity and dielectric susceptibility measured by Allakhverdiev *et al* [18], Aldzhanov *et al* [19] and Mikailov *et al* [20] in this temperature range. At the same time, Mikailov *et al* [20] interpreted their dielectric data on $TlGaSe_2$ below T_c, suggesting a coexistence of at least two polar sublattices with different dielectric relaxation behaviors. The above results are in accord with our NMR findings. A study of phase transitions by Fradkin [51] showed that the coupling between the elastic strain and the order parameter causes the transformation to be preceded in a finite temperature interval with the equilibrium volume fraction dependent on temperature. Such a scenario may also be relevant to our data.

Second, let us discuss the anomaly in ^{205}Tl spin–lattice relaxation around 128 K that, at first sight, may indicate a phase transition. One can find, however, that the ^{69}Ga spectra (figure 7) and the temperature dependences of the ^{69}Ga resonance frequency (figure 8) and of the ^{69}Ga spin–lattice relaxation time T_1 (figure 9) show no anomalies around 128 K. Therefore the observed maximum in T_1(^{205}Tl) around 128 K is not due to a phase transition.

Third, let us compare the temperature dependences of the spin–lattice relaxation time for ^{69}Ga and ^{205}Tl nuclei. On approaching T_i from above, starting from ∼175 K, the relaxation time T_1 of the ^{69}Ga nuclei decreases as expected for a spin–lattice relaxation mechanism dominated by a soft mode [52]. One can speculate that this soft mode mainly concerns dynamics of the $GaSe_4$ tetrahedra rather than Tl ions. The corresponding maximum of T_1 of the ^{205}Tl nuclei is observed at much lower temperature, around 128 K, and is accompanied by a reduction in T_1 on further cooling and approaching phase transition from above, also reflecting soft mode behavior [52]. The observed critical behavior is typical of a second-order phase transition. We note that the phase transition at $T_i = 118$ K has been repeatedly detected by means of dielectric [12, 13], specific heat [14, 17, 22] and diffraction [14–16] measurements and was shown to be a second-order transition, in accordance with our findings.

Distribution of the spin–lattice relaxation times, and, correspondingly, of the correlation times of critical fluctuations on approaching phase transition at T_i, observed in the ^{69}Ga spin–lattice relaxation measurements in the temperature range from 118 to 128 K, is probably due to some inhomogeneity of the crystal, which is presumably caused by a coexistence of some spatially dispersed local regions in the crystal. This may be caused by stacking faults of the layers, for example. One can also speculate that the inhomogeneity may reflect a relaxor-like behavior above T_i. Such a behavior has recently been reported for the doped and γ-irradiated $TlInS_2$ [53] that is isostructural to $TlGaSe_2$. In our crystal, such an effect may be caused by defects and crystal imperfections, causing inhomogeneous local ordering in the paraelectric phase.

We note that exciton spectroscopy and dielectric measurements of $TlGaSe_2$ made by Alekperov [54] within the temperature range corresponding to the paraelectric–ferroelectric phase transition and its vicinity, allowed him to consider the crystal as consisting of two or more spatially dispersed media with different dielectric constants and somewhat different behavior. This result is in accord with our NMR findings.

We would also like to note that the $T_1(T)$ dependence for the ^{69}Ga nuclei (figure 9) exhibits a small dip around 210 K, just at the temperature which corresponds to the transformation seen in the ^{205}Tl NMR spectra.

5. Summary

In summary, our ^{69}Ga and ^{205}Tl NMR study of the $TlGaSe_2$ single crystal shows that the transformation from the high temperature paraelectric phase to the low temperature ferroelectric phase exhibits successive phase changes and occurs via the incommensurate phase that exists in the temperature range from $T_c = 107.5$ to $T_i = 118$ K. On approaching phase transition at T_i from above, the crystal exhibits soft mode behavior, which is different for Tl and Ga substructures. Several other spectra transformations observed in the experiments are not characteristic of phase transitions. Redistribution of ^{69}Ga line intensities with temperature in the ferroelectric phase indicates a variation of the domain structure and domain repartition in this phase. The Ga sublattice also reveals a distribution of the correlation times of critical fluctuations on approaching T_i from above, between ∼128 and 118 K, probably due to some stacking faults of the layers.

References

[1] Müller D and Hahn H 1978 *Z. Anorg. Allg. Chem.* **438** 258
[2] Henkel W, Hochheimer H D, Carlone C, Werner A, Yes S and von Schnering H G 1982 *Phys. Rev.* B **26** 3211
[3] Gasanly N M, Marvin B N, Sterin Kh E, Tagirov V I and Khalafov Z D 1978 *Phys. Status Solidi* b **86** K49
[4] Kalkan N, Hanias M P and Anagnostopoulos A N 1992 *Mater. Res. Bull.* **27** 1329
[5] Hanias M P and Anagnostopoulos A N 1993 *Phys. Rev.* B **47** 4261
[6] Hanias M P, Anagnostopoulos A N, Kambas K and Spyridelis J 1991 *Phys. Rev.* B **43** 4135
[7] Hanias M P, Kalomiros J A, Karakotsou Ch, Anagnostopoulos A N and Spyridelis J 1994 *Phys. Rev.* B **49** 16994
[8] Watzke O, Schneider T and Martienssen W 2000 *Chaos Solitons Fractals* **11** 1163
[9] Gorelik V S, Agal'tsov A M and Ibragimov T D 1988 *J. Appl. Spectrosc.* **51** 661
[10] Ibragimov T D and Aslanov I I 2002 *Solid State Commun.* **123** 339
[11] Aliyev V P, Babayev S S, Mammadov T G, Seyidov M-H Y and Suleymanov R A 2003 *Solid State Commun.* **128** 25
[12] Volkov A A, Goncharov Yu G, Kozlov G V, Lebedev S P, Prokhorov A M, Aliev R A and Allahverdiev K P 1983 *Pis. Zh. Eksp. Teor. Fiz.* **37** 517 (in Russian)
Volkov A A, Goncharov Yu G, Kozlov G V, Lebedev S P, Prokhorov A M, Aliev R A and Allahverdiev K P 1983 *JETP Lett.* **37** 615 (Engl. Transl.)
[13] Volkov A A, Goncharov Yu G, Kozlov G V and Sardarly R M 1984 *Pis. Zh. Eksp. Teor. Fiz.* **39** 293 (in Russian)
Volkov A A, Goncharov Yu G, Kozlov G V and Sardarly R M 1984 *JETP Lett.* **39** 351 (Engl. Transl.)
[14] Hochheimer H D, Gmelin E, Bauhofer W, von Schnering-Schwarz C, Schnering H G, Ihringer J and Appel W 1988 *Z. Phys.* B **73** 257
[15] McMorrow D F, Cowley R A, Hatton P D and Banys J 1990 *J. Phys.: Condens. Matter* **2** 3699
[16] Kashida S and Kobayashi Y 1998 *J. Korean Phys. Soc.* **32** S40 (Suppl., Proc. 9th Int. Mtg on Ferroelectricity, 1997, Pt. 1)
[17] Abdullaeva S G, Abdullaev A M, Mamedov K K and Mamedov N T 1984 *Sov. Phys.—Solid State* **26** 375
[18] Allakhverdiev K R, Aldzanov M A, Mamedov T G and Salaev E Yu 1986 *Solid State Commun.* **58** 295
[19] Aldzhanov M A, Guseinov N G and Mamedov Z N 1987 *Phys. Status Solidi* a **100** K145
[20] Mikailov F A, Basaran E, Senturk E, Tumbek L, Mammadov T G and Aliev V P 2004 *Solid State Commun.* **129** 761
[21] Abutalybov G I, Larionkina L S and Ragimova N A 1989 *Sov. Phys.—Solid State* **31** 312
[22] Mamedov N T, Krupnikov E S and Panich A M 1989 *Fiz. Tverd. Tela* **31** 290 (in Russian)
Mamedov N T, Krupnikov E S and Panich A M 1989 *Sov. Phys.—Solid State* **31** 159 (Engl. Transl.)
[23] Panich A M, Gabuda S P, Mamedov N T and Aliev S N 1987 *Fiz. Tverd. Tela* **29** 3694 (in Russian)
Panich A M, Gabuda S P, Mamedov N T and Aliev S N 1987 *Sov. Phys.—Solid State* **29** 2114 (Engl. Transl.)
[24] Panich A M 2004 *Appl. Magn. Reson.* **27** 29
[25] Panich A M and Gasanly N M 2001 *Phys. Rev.* B **63** 195201
[26] Panich A M and Kashida S 2002 *Physica* B **318** 217
[27] Kholopov E V, Panich A M and Kriger Yu G 1983 *Zh. Teor. Exp. Phys.* **84** 1091 (in Russian)
Kholopov E V, Panich A M and Kriger Yu G 1983 *Sov. Phys.—JETP* **57** 632 (Engl. Transl.)
[28] Panich A M 1989 *Fiz. Tverd. Tela* **31** 279 (in Russian)
Panich A M 1989 *Sov. Phys.—Solid State* **31** 1814 (Engl. Transl.)
[29] Panich A M and Doert Th 2000 *Solid State Commun.* **114** 371
[30] Kholopov E V, Panich A M and Kriger Yu G 1986 *Phys. Status Solidi* b **137** K121
[31] Mamedov N T and Panich A M 1990 *Phys. Status Solidi* a **117** K15
[32] Panich A M and Kashida S 2004 *J. Phys.: Condens. Matter* **16** 3071
[33] Panich A M, Teske C L, Bensch W, Perlov A and Ebert H 2004 *Solid State Commun.* **131** 201
[34] Panich A M, Teske C L and Bensch W 2006 *Phys. Rev.* B **73** 115209
[35] Kashida S, Yanadori Y, Otaki Y, Seki Y and Panich A M 2006 *Phys. Status Solidi* a **203** 2666
[36] Slichter C P 1978 *Principles of Magnetic Resonance* (Berlin: Springer)
[37] Landau L and Lifshitz E 1963 *Quantum Mechanics* (Moscow: Fizmatgiz)
[38] Panich A M 1999 *Synth. Met.* **100** 169
[39] Blinc R 1981 *Phys. Rep.* **79** 331
[40] Blinc R, Prelovsek P, Rutar V, Seliger J and Zumer S 1986 *Incommensurate Phases in Dielectrics* vol 1, ed R Blinc and A P Levanyuk (Amsterdam: North-Holland)
[41] Panich A M, Zemnukhova L A and Davidovich R L 2001 *J. Phys.: Condens. Matter* **13** 1609
[42] Abragam A 1961 *The Principles of Nuclear Magnetism* (Oxford: Clarendon) chapter VIII, p 314
[43] Andrew E R and Tunstall D P 1961 *Proc. Phys. Soc.* **78** 1
[44] Kranendonk J van 1954 *Physica* **20** 781
[45] Yosida K and Moriya T 1956 *J. Phys. Soc. Japan* **11** 33
[46] Kondo J and Yamashita J 1959 *J. Phys. Chem. Solids* **10** 245
[47] Pound R V 1950 *Phys. Rev.* **79** 685
[48] Goldburg W I 1959 *Bull. Am. Phys. Soc.* II **4** 252
[49] Andrew E R and Swanson K M 1960 *Proc. Phys. Soc.* **75** 582
[50] Phillips J C 1996 *Rep. Prog. Phys.* **59** 1133
[51] Fradkin M A 1997 *J. Phys.: Condens. Matter* **9** 7925
[52] Blinc R and Žekš B 1974 *Soft Modes in Ferroelectrics and Antiferroelectrics* (Amsterdam: North-Holland)
[53] Sardarly R M, Mamedov N T, Wakita K, Shim Y, Nadjafov A I, Samedov O A and Zeynalova E A 2006 *Phys. Status Solidi* a **203** 2845
[54] Alekperov O Z 2003 *J. Phys. Chem Solids* **64** 1707